Fermilab FERMILAB-CONF-07-008-AD January 2007

MARS15 Overview[1]

N.V. Mokhov and S.I. Striganov[2]

Fermilab, Batavia, IL 60510, U.S.A.

Abstract. MARS15 is a Monte Carlo code for inclusive and exclusive simulation of three-dimensional hadronic and electromagnetic cascades, muon, heavy-ion, and low-energy neutron transport in accelerator, detector, spacecraft, and shielding components in the energy range from a fraction of an electronvolt up to 100 TeV. Main features of the code are described in this paper with a focus on recent developments and benchmarking. Newest developments concern inclusive and exclusive nuclear event generators, extended particle list in both modes, heavy-ion capability, electromagnetic interactions, enhanced geometry, tracking, histograming and residual dose modules, improved graphical-user interface, and other external interfaces.

Keywords: Hadrons, cascades, Monte Carlo, simulation
PACS: 13.85.-t, 24.10.Lx

INTRODUCTION

The MARS code system [1] is a set of Monte Carlo programs for detailed simulation of hadronic and electromagnetic cascades, muon, heavy-ion, and low-energy neutron transport in an arbitrary 3-D geometry of shielding, accelerator, detector, and spacecraft components with energy ranging from a fraction of an electronvolt up to 100 TeV. It has been developed since 1974 at IHEP, SSCL and Fermilab. The current MARS15 version combines the well established theoretical models for strong, weak and electromagnetic interactions of hadrons, heavy ions and leptons with a system which can contain up to 10^5 objects, ranging in dimensions from microns to hundreds of kilometers in the same run. A setup can be made of up to 100 composite materials (those from 165 built-in or any user-defined), in presence of arbitrary 3-D magnetic and electric fields. A powerful user-friendly graphical-user interface (GUI) is used for visualization of geometry, materials, fields, particle trajectories, and results of calculations. MARS15 has five geometry options and flexible histograming options, can use MAD optics files as an input through a powerful MAD-MARS Beam Line Builder, and provides an MPI-based multiprocessing option, with various tagging, biasing and other variance reduction techniques.

There are quite substantial improvements in most of the code modules of the current version compared to those documented earlier. Some highlights are given below on the list of elementary particles and arbitrary heavy ions, their interaction cross-sections, inclusive and exclusive nuclear event generators, photohadron production, correlated

---

[1] Presented paper at the Hadronic Shower Simulation Workshop, September 6-8, 2006, Fermilab.

[2] Work supported by Fermi Research Alliance, LLC, under contract No. DE-AC02-07CH11359 with the U.S. Department of Energy.

ionization energy loss and multiple Coulomb scattering, nuclide production, residual activation, and radiation damage (DPA). In particular, the details of a new model for leading baryon production and implementation of advanced versions of the Cascade-Exciton Model (CEM03) as well as the Los Alamos version of the Quark-Gluon String Model (LAQGSM03) are given.

Many people participated in the MARS code development over its 33-year history. Current contributors are N.V. Mokhov, S.I. Striganov, K.K. Gudima, C.C. James, M.A. Kostin, S.G. Mashnik, M.E. Monville, N. Nakao, I.L. Rakhno, and A.J. Sierk. Growing demand, diversity of applications and invaluable feedback from 300 MARS users worldwide motivate continuous developments of the code.

PARTICLES AND NUCLEAR CROSS-SECTIONS

A list of particles transported by MARS15 is extended to include neutral kaons, antineutrons and hyperons/antihyperons totaling in more than 40 species, all with their corresponding cross-sections, decay modes and electromagnetic processes. Arbitrary heavy ions with atomic mass A and charge Z are now fully treated by the code, including decays of unstable ions.

Total and elastic cross-sections of hadron-nucleon interactions for ordinary hadrons are described using corresponding fits to experimental data. Cross-sections for hyperon-nucleon interactions are described via the ordinary hadron cross-sections using the Additive Quark Model rules. At energies above 5 GeV, such an approach agrees well with data. At lower energies, the hyperon-nucleon cross-sections are very close to proton-nucleon ones. Hadron-nucleus total and inelastic cross-sections at energies above 5 GeV are calculated using the Glauber model. At lower energies, parameterizations to experimental data are used. For neutral kaons, cross-sections on both nucleon and nucleus targets are calculated using the relation based on an isospin and hypercharge conjugation. Total and inelastic cross-sections for heavy-ion nuclear interactions are based on the JINR model (see Ref. [2]). Photonuclear interaction cross-sections are described in great detail for all nuclei and energies from a few MeV up to 40 TeV using approximations from Ref. [3]. Fig. 1(a) gives an example of the neutron and heavy-ion cross-section descriptions in the code.

INCLUSIVE EVENT GENERATOR

The basic model for the original MARS program, introduced in 1974, came from Feynman's ideas concerning an inclusive approach to multiparticle reactions and *weighting* techniques. At each interaction vertex, a particle cascade tree can be constructed using only a fixed number of representative particles (the precise number and type depend on the specifics of the interaction), and each particle carries a statistical weight w, which is equal, in the simplest case, to the partial mean multiplicity of the particular event. Energy and momentum are conserved *on average* over a number of collisions. It was proved rigorously that such an estimate of the first moment of the distribution function is unbiased [5].

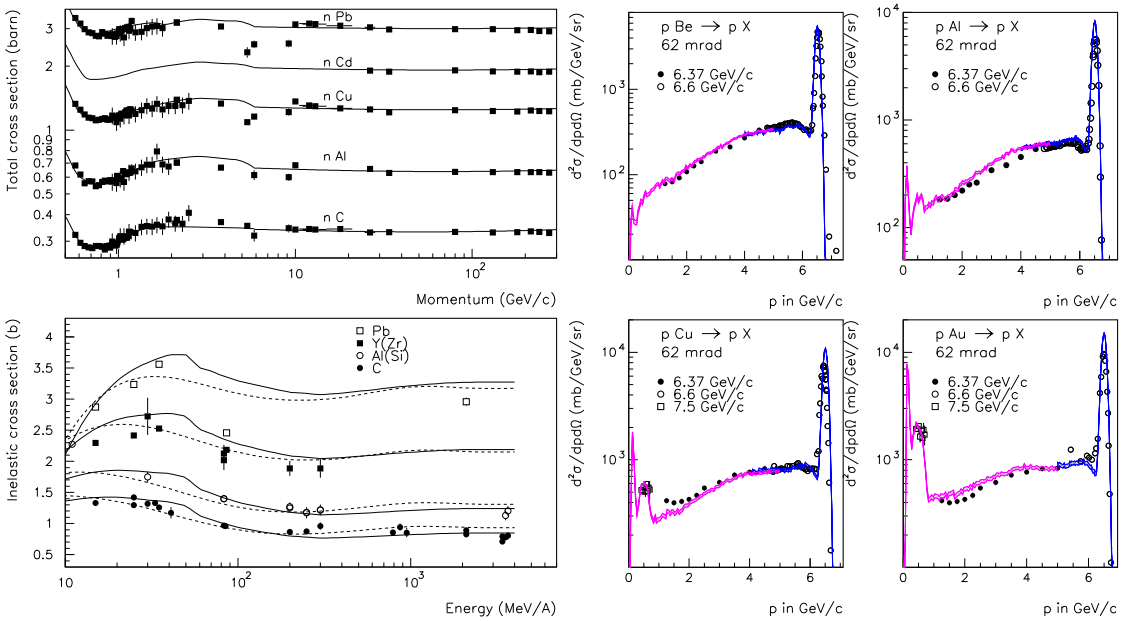

FIGURE 1. **Left:** Total neutron-nucleus cross-sections (top) and inelastic nuclear cross-sections of ^{12}C ions (bottom) as calculated in MARS15 (solid lines) *vs* data [4]; dashed lines are from a NASA model. **Right:** Invariant cross-sections for $pA \to pX$ reactions at 6.37 to 7.5 GeV/c on various nuclei in MARS15 (lines) *vs* data [6].

Inclusive particle production in nuclear interactions above 3 GeV is modeled in MARS15 using the following form for double differential distributions (taking $pA \to pX$ reaction as an example):

$$\frac{d^2N^{pA\to pX}}{dpd\Omega} = R^{pA\to pX}(A,E_0,p,p_\perp)\frac{d^2N^{pp\to pX}}{dpd\Omega} + F_{qel} + F_{ce}.$$

Differential cross-sections on a hydrogen target are described by a set of models and phenomenological formulae. For example, proton production in pp-collisions $\frac{d^2N^{pp\to pX}}{dpd\Omega}$, is described with a high accuracy in four kinematic regions of Feinman $x_F = |p_L^*/p_{max}^*|$:

1. Resonance region $x_F > 1 - 2.2/p_0$: a sum of five baryon resonances, Breit-Wigner formulae.
2. Diffractive dissociation region $1 - 2.2/p_0 < x_F < 0.9$: a triple-Reggeon formalism.
3. Fragmentation region $0.4 < x_F < 0.9$: a phenomenological model with a flat behavior on longitudinal and exponential one on transverse momenta.
4. Central region $0 < x_F < 0.4$: a fit to experimental data with normalizations at $x_F = 0$ and $x_F = 0.4$.

A nuclear modification factor $R^{pA\to pX}$ is known much better than the absolute yields, and its dependence on particle momenta $p_\perp$, p_0 and p is much weaker than for the differential cross-sections themselves. For $pA \to pX$, it is presented in a factorized form

$$R^{pA\to pX} = F(p/p_0)\left(\frac{A}{2}\right)^{\alpha p_T^2}\left(\frac{A}{9}\right)^{\gamma(E_0)},$$

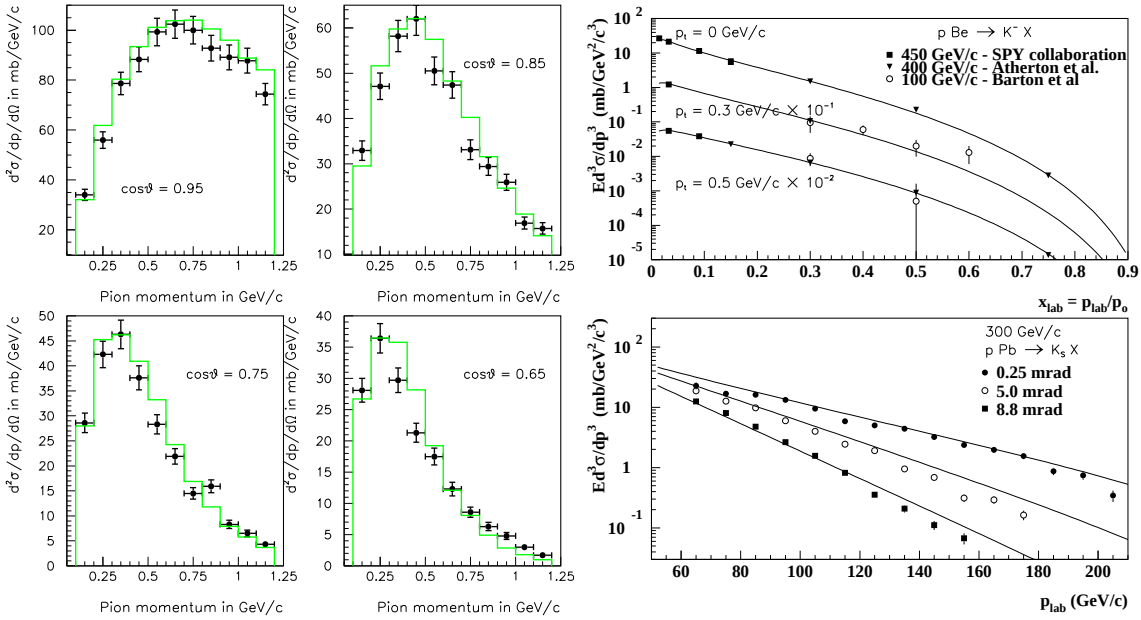

FIGURE 2. Invariant cross-sections for $pBe \rightarrow \pi^- X$ at 12.3 GeV/c [7] (left), $pBe \rightarrow K^- X$ at 100 to 450 GeV/c [8] and $pPb \rightarrow K_s X$ at 300 GeV/c [9] (right) *vs* MARS15; symbols are data and lines are calculations.

with a momentum dependence given by the Additive Quark Model. Appropriate formulae are used in the corresponding kinematic regions for meson production.

For all projectiles and secondary particles, quasi-elastic scattering (F_{qel}) and Fermi-motion are additionally simulated in this inclusive model and supplied with new phenomenological models for cascade/evaporation (F_{ce}), fission, and anti-nucleon production processes. Pion and charged kaon production phenomenological models have been improved. Recent additions to the inclusive event generator also include coupled nucleon / anti-nucleon production, neutral kaon production and heavy-ion nuclear interactions according to a superposition model. The later is used only for simplified non-exclusive modeling in a non-LAQGSM mode (see next section). A quality of the model for protons, pions and kaons is demonstrated in Fig. 1b, Fig. 2a and Fig. 2b, respectively.

EXCLUSIVE EVENT GENERATOR

A substantially improved Cascade-Exciton Model code, CEM03.01 [10] combined with the Fermi break-up model, the coalescence model, an improved version of the Generalized Evaporation-fission Model (GEM2), and a recent multi-fragmentation extension is used in MARS15 as a default for hadron-nucleus interactions below 5 GeV. It is a completely new, updated and modified version in comparison with its predecessors, not just an incremental improvement. CEM03.01 describes reactions induced by nucleons, pions and photons as a three-stage process: Intra-Nuclear Cascade (INC), followed by pre-equilibrium emission of particles during the de-excitation of the excited residual nuclei formed during the INC, followed by evaporation of particles from or fission of

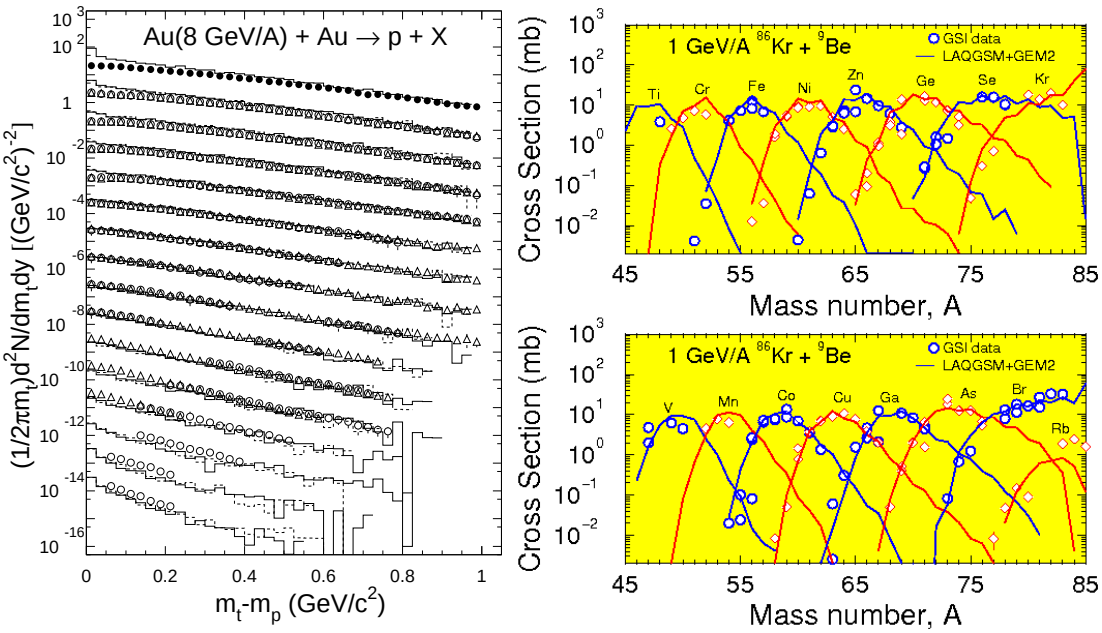

FIGURE 3. Left: Invariant proton yields per central $Au + Au$ collision at 8 GeV/A as calculated in MARS15 with LAQGSM03 (histograms) *vs* experiment [13]; solid lines and open circles is forward production, dashed lines and open triangles is backward production; mid-rapidity (upper set) is shown unscaled, while the 0.1 unit rapidity slices are scaled down by successive factors of 10. **Right:** Mass yield for $^{86}Kr + ^{9}Be$ as calculated with LAQGSM03 (lines) and measured in Ref. [14].

the compound nuclei. If the excited residual nucleus produced after the INC has a mass number $A < 13$, CEM03.01 uses a recently updated and improved version of the Fermi Break-up model to calculate its decay instead of considering a pre-equilibrium stage followed by evaporation from compound nuclei. CEM03.01 considers also coalescence of complex particles up to ^{4}He from energetic nucleons emitted during the INC.

The Los Alamos Quark-Gluon String Model code, LAQGSM03 [11], is implemented into MARS15 for particle and heavy-ion projectiles at 10 MeV/A to 800 GeV/A, including π^--capture and annihilation at rest. This provides a power of full theoretically consistent modeling of exclusive and inclusive distributions of secondary particles as well as spallation, fission, and fragmentation products. For quite some time, MARS has used the Dual-Parton Model code, DPMJET3 [12], for the very first vertex in a cascade tree. This is used in our numerous studies for the LHC 7×7 TeV collider and its detectors, and at very high energies up to 100 TeV. Fig. 3 shows results of MARS15/LAQGSM benchmarking at 1 and 8 GeV/A for proton and nuclide production in heavy-ion nuclear interactions.

ELASTIC SCATTERING AND LOW-ENERGY NEUTRONS

The elastic model at E<5 GeV is based on evaluated nuclear data from the LA-150 and ENDF/HE-VI libraries and from other sources (see Ref. [15]). For protons, the interference of nuclear and Coulomb elastic scattering is taken into account. At E>5 GeV, a

simple analytical description used in the code for the coherent component of scattering cross-sections is quite consistent with data.

Once the energy of neutrons falls below 14 MeV during shower development, all subsequent neutron interactions are described using the appropriate MCNP4C [16] modules. Secondaries generated at this stage by neutrons – protons, photons and deuterons – are directed back to the MARS15 modules for a corresponding treatment. This implementation, along with algorithms developed for heavier recoils and photons from the thermal neutron capture on ^{6}Li and ^{10}B, allows the detailed description of corresponding effects in hydrogenous, borated and lithium-loaded materials. The interface includes several other modifications to the dynamically allocated storage, material handling, as well as an optional writing of low-energy neutrons and other particles to a file for processing at a later time.

ELECTROMAGNETIC PROCESSES, MUONS AND NEUTRINOS

The mean ionization energy loss for charged particles, except for heavy ions, is calculated using the Bethe formalism with the density correction. For heavy ions – as described in Ref. [2] – the Lindhard-Sorensen correction to the regular ionization logarithm and a Barkas term are taken into account. In addition, at low ion energies, the processes of electron capture and loss are accounted for by means of an effective ion charge. The effective charge, z_{eff}, is determined according to semi-empirical formulae and used instead of a bare ion charge. The projectile nuclear form-factor is also taken into account.

A further improved algorithm [17] for modeling correlated ionization energy loss and multiple Coulomb scattering is used in MARS15 for arbitrary mixtures. It takes into account arbitrary projectile and nuclear target charge distributions, exact kinematics of projectile-electron interactions, nuclear screening, and projectile-electron interactions. It accurately treats both soft and hard collisions. Calculated correlations between energy loss and scattering are quite substantial for low-Z targets. Radiative processes for single-charged particles and heavy ions – bremsstrahlung and direct pair production – are modeled directly [18].

Analog or inclusive simulation algorithms are used for prompt muon production (single muons in charmed meson decays, $\mu^+\mu^-$ pairs in vector meson decays, and the dimuon continum), Bethe-Heitler $\mu^+\mu^-$ pairs and direct $e^+e^- \to \mu^+\mu^-$ annihilation. Neutrinos from meson and muon decays can be forced to interact with matter through all the possible mechanisms.

NUCLIDE INVENTORY, RESIDUAL DOSE AND DPA

Mass and charge number distributions (1D and 2D) are calculated in MARS15 for nuclides generated in arbitrary materials and regions of a setup studied. A further improved ω-factor based algorithm [19] to calculate residual dose rates in arbitrary composite materials for arbitrary irradiation and cooling times is used in MARS15. The algorithm distinguishes three major energy groups responsible for radionuclide production [1]: (1) above 20 MeV, (2) 1 to 20 MeV and (3) below 0.5 eV. Creation

of the residual nuclides was pre-calculated with the FLUKA code. The emission rates of de-excitation photons are determined for irradiation time 12 hours$< T_i <$20 years and cooling time 1 sec$< T_c <$20 years. Corresponding dose rates on the outer surfaces are calculated from photon fluxes and related to the star density above 20 MeV (first group) and neutron fluxes in two other energy groups. A new algorithm [20] is used to calculate residual dose on very small objects as well as its attenuation in air around. Radiation damage to material – displacements per atom (DPA) – is calculated in MARS15 within a damage energy concept, taking into account recoil nuclei in elastic and inelastic nuclear interactions.

BIASING, VARIANCE REDUCTION AND TAGGING

Many processes in MARS15, such as electromagnetic showers, most hadron-nucleus interactions, decays of unstable particles, emission of synchrotron photons, photohadron production, and muon pair production, can be treated either analogously or inclusively with corresponding statistical weights. The choice of method is left for the user to decide, via the input settings. Other variance reduction techniques used in MARS15 are weight-window, splitting and Russian roulette, exponential transformation, probability scoring, and step/energy cutoffs. The goal here is to maximize computing efficiency t_0/t, where t is the CPU time needed to get a RMS error σ equal to the one in the reference method with the CPU time t_0 provided $\sigma < 20\%$. In addition to a standard multi-parameter bias setting in the code, a new user-friendly global bias control was recently introduced via a single card BIAS with parameters which define exclusive/inclusive switch, Russian Roulette and/or exponential transform control for six processes: decays of unstable particles, prompt muon production, Bethe-Heitler muon production, $e^+e^- \to \mu^+\mu^-$ annihilation, photo-nuclear reactions, and anti-proton production.

A further enhanced tagging module in MARS15 allows one to tag the origin of a given signal/tally: geometry, process and phase-space. It is invaluable in studying a source term and for sensitivity analysis. A user-friendly access is provided to the process ID at a scoring (histograming) stage, giving flags to 50 process types.

GEOMETRY AND MATERIALS

MARS15 provides a user with five geometry description options:

1. *Standard*: heterogeneous R-Z-ϕ cylinder.
2. *Non-standard*: arbitrary geometry defined by a user in a Fortran or C routine.
3. *Extended*: a set of contiguous or overlapping geometrical shapes, currently, boxes, spheres, cylinders, truncated cones, tetrahedra, and elliptical tubes. Each shape can be sub-divided into many sub-regions in each direction; arbitrary transformation matrices can be applied to any object.
4. *MCNP*: read in an input geometry description in the MCNP format.
5. *FLUKA*: read in an input geometry description in the FLUKA format.

Any or all of the five geometry options can be used simultaneously (co-exist) in a setup description. An arbitrary number of regions can be used, with a default maximum of 10^5. Volumes of all regions are auto-calculated for the predefined shapes. A short Monte-Carlo session of the code is used to calculate volumes of complex and overlapped regions. A corresponding output file provides calculated volumes with statistical errors and is directly linked to the main code.

The *extended* geometry provides exact crossing of particle tracks with the surfaces that prevents small regions within a large volume from being skipped over. In the other four options, boundary localization is based on an iterative algorithm and user needs to take care of appropriate region numbering, pilot steps and localization parameters.

A list of the built-in materials in MARS15 includes 165 elements and composites. Recently added are many kinds of steel, cast iron, mineral oil, gadolinium-loaded scintillator, etc. On top of that, customized composites can be defined in a user routine. The code does a separate treatment of gaseous and liquid states.

TRACKING AND HISTOGRAMING

Particle tracking – in a magnetic field with Coulomb scattering and energy loss for charged particles and decays for unstable particles – and histograming algorithms, which are already quite sophisticated, have further been refined to assure the highest accuracy and CPU performance. Slowing down pion and muon decays and nuclear capture are carefully modeled in a competition.

Performance of scoring algorithms for volume and surface detectors linked to the geometry was further improved. A further developed user-friendly flexible XYZ-histograming module allows scoring numerous distributions – total and partial particle fluxes, star density, total and partial energy deposition, DPA, temperature rise, prompt and residual dose rates, particle spectra, etc. – in boxes arbitrary positioned in a 3D system, independent of geometry description (mesh tally). Its performance and accuracy were also recently improved.

GUI AND MULTIPROCESSING

The existing Tcl/Tk-based 2D MARS-GUI-SLICE functionality was further improved and extended, which further extends the power of visualization of the modeled system: geometry, materials and magnetic field descriptions, simulated processes, and calculated results. New features include: selection of four GUI window sizes, online renormalization of histograms displayed, extended information on particle ID and histogram values at a point, switchable canvas aspect ratios, switchable format of a saved plot, etc. Arbitrary 3-D rotation of a slice is possible.

Since 2004, parallel processing is default in all CPU-hungry applications of MARS15 [1]; it is based on the Message Passing Interface (MPI) libraries. Parallelization is job-based, i.e. the processes, replicating the same geometry of the setup studied, run independently with different initial seeds. A unique master process – also running event histories – collects intermediate results from an arbitrary number

of slaves and calculates the final results when a required total number of events has been processed. Intermediate results are sent to the master on its request generated in accordance with a scheduling mechanism. The performance scales almost linearly with the number of nodes used (up to tens of nodes at Fermilab clusters).

BEAM-LINE BUILDER

The MAD-MARS Beam-Line Builder (MMBLB) is the interface system [21, 22] to build beam-line and accelerator models in the MARS format. MMBLB reads in a MAD lattice file and puts the elements in the same order into MARS. Each element is assigned six functions: element type/name, geometry, materials, field, volume and initialization. MMBLB has been substantially extended [23]:

- The set of supported element types includes now almost all the elements supported by MAD.
- An arbitrary number of beam lines – arbitrary positioned and oriented – can be put in a MARS15 model.
- More sophisticated algorithms and new data structures enable more efficient searches through the beam line geometry.
- Tunnel geometry can now follow the beam line or be described independently of it.

MMBLB is heavily used in numerous MARS15 accelerator and machine-detector interface applications at Tevatron, LHC, J-PARC, and ILC. Fig. 4 shows just two recent examples of MARS15 use: muon fluxes in a 550-m region upstream of the LHC CMS detector due to 7-TeV proton interactions with residual gas, and photon tracks generated in the 220-m extraction line after 250×250-GeV e^+e^- collisions at the ILC IP. MMBLB and the GUI described above were used here to describe geometry, materials and magnetic fields, debug the model, perform MARS15 runs, and display results calculated.

BENCHMARKING

Debugging, validation and comparisons are done for the MARS code continuously once a new model or algorithm is implemented, a new problem is attacked, or a colleague provides interesting results from his/her code. Numerous verifications were performed at Fermilab over the last two decades in accelerator, shielding, targetry, and detector applications. Recent verifications of MARS15 by the authors and the MARS community were presented at the workshop [24, 25]. They prove the MARS15 code reliability, flexibility and robustness on microscopic and macroscopic levels.

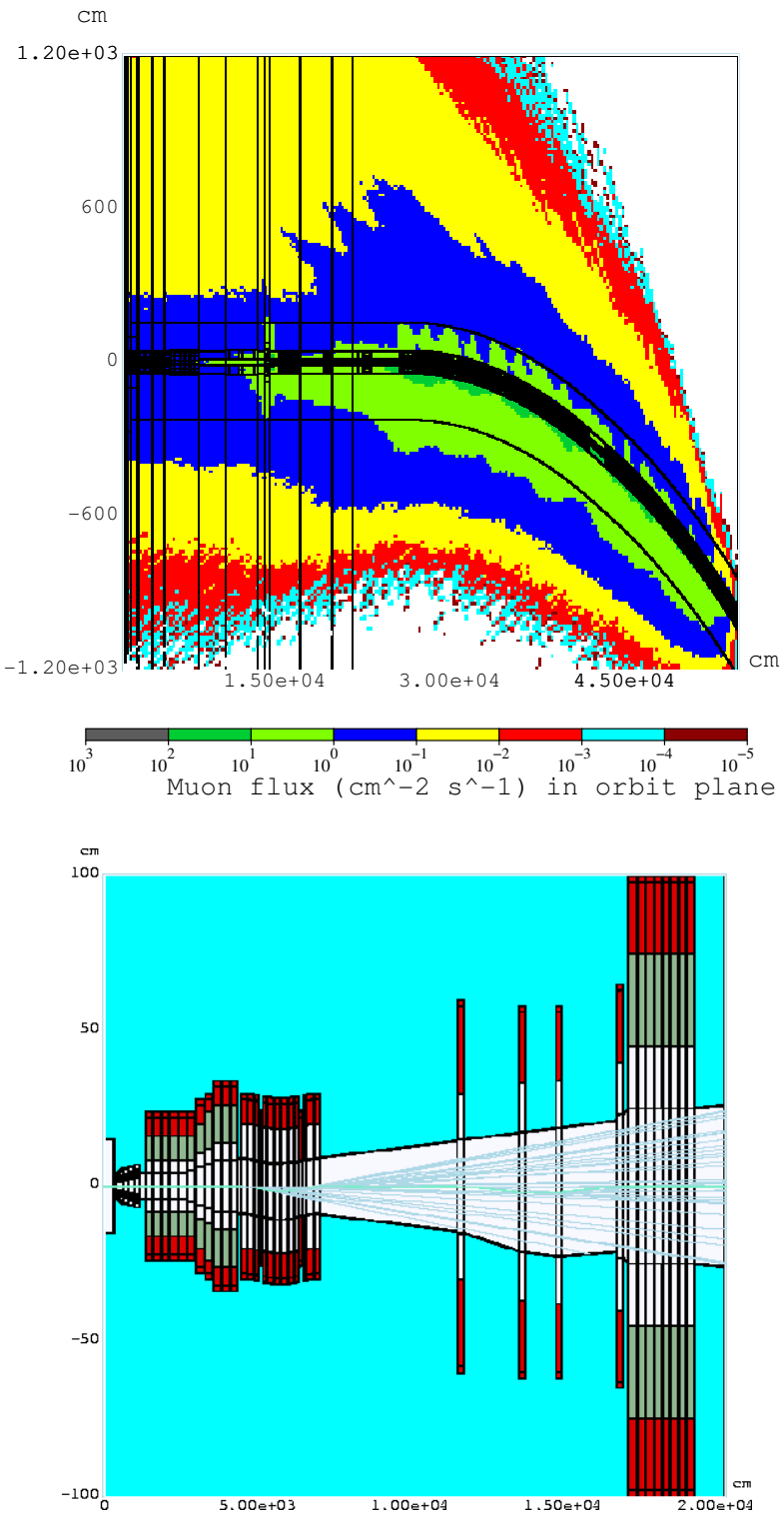

FIGURE 4. Muon flux isocontours in the LHC IP5 due to beam-gas interactions (top) and photons generated in the ILC 18-MW extraction line (bottom).

REFERENCES

1. N.V. Mokhov, *Fermilab-FN-628* (1995); N.V. Mokhov et al, *Rad. Prot. Dosimetry*, **116**, 99 (2005); N.V. Mokhov et al, *Int. Conf. on Nucl. Data Sci. Technology, AIP Conf. Proc.*, **769**, 1618 (2005); http://www-ap.fnal.gov/MARS/.
2. N.V. Mokhov et al, *Rad. Prot. Dosimetry*, **116**, 104 (2005).
3. M.V. Kossov, *Eur. Phys. J.*, **A14**, 377 (2002).
4. V.S. Barashenkov, "Cross-Sections of Particle and Nuclei Interactions with Nuclei", JINR, Dubna, Russia (1993).
5. , A.N. Kalinovskii, N.V. Mokhov and Yu.P. Nikitin, "Passage of High-Energy Particles through Matter", AIP, New York (1989).
6. A.S. Arefiev et al, ITEP-85-25 (1985); L.Z. Barabash et al, *Sov. J. Nucl. Phys.* **36**, 90 (1982); Yu.D. Bayukov et al, *Sov. J. Nucl. Phys.* **42**, 116 (1985).
7. I. Chemakin et al, *Phys. Rev.* , **C65:024904** (2002).
8. G. Ambrosini et al, *Eur. Phys. J.*, **C10**, 605 (1999); H.W. Atherton et al, CERN 80-07 (1980); D.S. Barton et al, *Phys. Rev.*, **D27**, 2580 (1983).
9. P.L. Skubic et al, *Phys. Rev.*, **D18**, 3115 (1978).
10. S.G. Mashnik et al, "CEM03.01 User Manual", LANL LA-UR-05-7321 (2005).
11. K.K. Gudima et al, *LA-UR-01-6804* (2001).
12. http://sroesler.home.cern.ch/sroesler/dpmjet3.html.
13. J.L. Klay et al, *Phys. Rev. Lett.*, **88**, 102301 (2002).
14. Y. Iwata et al, *Phys. Rev.*, **C64**, 054609 (2001).
15. I.L. Rakhno, N.V. Mokhov, E. Sukhovitski, S. Chiba, *ANS Topical Meeting on Accelerator Applications/Accelerator Driven Transmutation Technology Applications, AccApp/ADTTA'01*, Reno, Nevada, Omnipress CD ROM (2002).
16. J.F. Briesmeister, "MCNP - A General Monte Carlo N-Particle Transport Code, Version 4C", *Pub. LA-13709-M* (2000).
17. S.I. Striganov, *Rad. Prot. Dosimetry*, **116**, 293 (2005).
18. N.V. Mokhov, S.I. Striganov, in *AIP Conf. Proc.*, **372**, 234-256 (1996).
19. I.L. Rakhno et al, "Benchmarking Residual Dose Rates in a NuMI-like Environment", in [15].
20. N.V. Mokhov, E.I. Rakhno, I.L. Rakhno, "Residual Activation of Thin Accelerator Components", *Fermilab-FN-0788-AD* (2006).
21. D.N. Mokhov et al, "MAD Parsing and Conversion Code", *Fermilab-TM-2115* (2000).
22. O.E. Krivosheev et al, "A Lex-based MAD Parser and its Applications", in *Proc. 2001 Particle Accel. Conf.*, 3036-3038, Chicago, June 2001.
23. M.A. Kostin, O.E. Krivosheev, N.V. Mokhov, I.S. Tropin, "An Improved MAD-MARS Beam-Line Builder: User's Guide", *Fermilab-FN-0738-rev* (2004).
24. N.V. Mokhov, S.I. Striganov, "Recent Verifications in MARS15", talk at the HSSW06 workshop.
25. N.V. Mokhov, S.I. Striganov, "Hadronic Shower Code Inter-Comparison and Verification", in these Proceedings.